Sparsity-Promoting Tomographic Fluorescence Imaging With Simplified Spherical Harmonics Approximation

Dong Han, Jie Tian*, *Fellow, IEEE*, Kai Liu, Jinchao Feng, Bo Zhang, Xibo Ma, and Chenghu Qin

***Abstract*—Fluorescence molecular tomography has become a promising technique for *in vivo* small animal imaging and has many potential applications. Due to the ill-posed and the ill-conditioned nature of the problem, Tikhonov regularization is generally adopted to stabilize the solution. However, the result is usually over-smoothed. In this letter, the third-order simplified spherical harmonics approximation to radiative transfer equation is utilized to model the photon propagation within biological tissues. Considering the sparsity of the fluorescent sources, we replace Tikhonov method with an iteratively reweighted scheme. By dynamically updating the weight matrix, L1-norm regularization can be approximated, which can promote the sparsity of the solution. Simulation study shows that this method can preserve the sparsity of the fluorescent sources within heterogeneous medium, even with very limited measurement data.**

***Index Terms*—Fluorescence imaging, optical imaging, tomography.**

I. Introduction

IN RECENT years, *in vivo* small animal molecular imaging has become an important method for biomedical research, and has many successful applications [1], [2]. Among molecular imaging modalities, fluorescence molecular tomography (FMT) is a promising technique that can three-dimensionally resolve the molecular processes by localizing the fluorescent probes based on certain inverse mathematical models.

Manuscript received April 15, 2010; revised May 24, 2010; accepted June 8, 2010. Date of publication June 21, 2010; date of current version September 15, 2010. This work was supported in part by the Project for the National Basic Research Program of China (973) under Grant 2006CB705700, in part by the Knowledge Innovation Project of the Chinese Academy of Sciences under Grant KGCX2-YW-907, in part by the Program for Changjiang Scholars and Innovative Research Team in University (PCSIRT) under Grant IRT0645, in part by the Chinese Academy of Sciences Hundred Talents Program. *Asterisk indicates corresponding author.*

D. Han, K. Liu, X. Ma, and C. Qin are with the Medical Image Processing Group, Institute of Automation, Chinese Academy of Sciences, Beijing 100190, China (e-mail: handong@fingerpass.net.cn; liukai@fingerpass.net.cn; maxibo@fingerpass.net.cn; qinch@fingerpass.net.cn).

*J. Tian is with the Medical Image Processing Group, Institute of Automation, Chinese Academy of Sciences, Beijing 100190, China, and also with the Life Science Research Center, School of Life Science and Technology, Xidian University, Xian 710071, China (e-mail: tian@ieee.org).

J. Feng is with the College of Electronic Information and Control Engineering, Beijing University of Technology, Beijing 100124, China (e-mail: fengjc@fingerpass.net.cn).

B. Zhang is with the Sino-Dutch Biomedical and Information Engineering School of Northeastern University, Shenyang 110004, China (e-mail: zhangbo@fingerpass.net.cn).

Color versions of one or more of the figures in this paper are available online at http://ieeexplore.ieee.org.

Digital Object Identifier 10.1109/TBME.2010.2053538

FMT is often an ill-posed inverse problem since only the photon distribution on the surface is measurable. This can be alleviated by increasing the measurement datasets. However, even if sufficient measurements can be obtained, the problem may still be ill-conditioned, which means that it is unstable and is sensitive to noises. To compute a meaningful approximate solution, Tikhonov regularization is generally incorporated to make the optimization problem less sensitive to perturbations. The advantage of Tikhonov regularization is that the optimization problem is simple and can be efficiently solved by now-standard minimization tools. However, the solution is often over-smoothed with the localized features lost during the reconstruction process [3].

To improve the quality of the reconstructed image, more *a priori* information should be included. Fortunately, for FMT problems, the domains of the fluorescent sources are often very small and sparse compared with the entire reconstruction domain [4]. This can be considered as valuable *a priori* information for FMT. A straightforward way to incorporate sparsity constraint is to replace the Tikhonov regularization with L0-norm regularization. However, the problem becomes NP-hard if L0-norm is utilized, and cannot be solved efficiently. Fortunately, it is proved that when the solution is sufficiently sparse, L0-norm can be replaced by L1-norm, which is convex and can be solved by standard optimization tools, such as pursuit algorithms [5]. Another advantage of L1-norm regularization is that it can still perform well when the measurement data is very limited. This has been well studied in the area of compressed sensing [6]. In recent years, several reconstruction algorithms for optical tomography problems with L1-norm regularization have been reported [4], [7], [8].

For FMT, another important issue is the accuracy of the photon-propagation model. Although the diffuse equation has been extensively utilized to describe photon propagation in biological tissues, yet it is not applicable in void or more absorptive regions. To resolve this problem, several improved models have been utilized, e.g., the discrete ordinates method (S_N) and the spherical harmonics approximation (P_N). However, the computational complexity is much higher. To reach a compromise between accuracy and efficiency, the simplified spherical harmonics approximation (SP_N) to radiative transfer equation (RTE) has been proposed, which is simpler than S_N and P_N with the same order [9]. Compared with the diffusion model, the SP_N model can significantly improve the solution in transport-like domains with high absorption and small geometries, which has been well demonstrated in [9]. In recent years, several papers

regarding SP_N-based optical tomography problems have been published [10], [11].

In this letter, an iteratively reweighted regularization method is proposed for the FMT problem with the third-order simplified spherical harmonics approximation (SP_3). Based on the basic idea of FOCUSS algorithm [12], we extend the Tikhonov method by incorporating a weighting matrix. By iteratively updating the weighting matrix, the L1-norm regularization can be approximated which tends to promote the sparsity of the solution. The advantage of the proposed method is that it can be easily incorporated into the existing iterative-reconstruction framework, and the extra work is merely the construction of the weighting matrix at each iteration, which is relatively cheap compared with the total reconstruction process. Reconstruction results on simulated data demonstrate the performance of the proposed method.

II. Method

A. Photon-Propagation Model

The SP_3 approximation model has the following form [9]:

$$\begin{cases} -\nabla\dfrac{\nabla\varphi_1(r)}{3\mu_{a1}(r)} + \mu_a(r)\varphi_1(r) - \dfrac{2\mu_a(r)}{3}\varphi_2(r) = S(r) \\ -\dfrac{2\mu_a(r)}{3}\varphi_1(r) - \nabla\dfrac{\nabla\varphi_2(r)}{7\mu_{a3}(r)} + \dfrac{4}{9}\mu_a(r)\varphi_2(r) \\ \quad + \dfrac{5}{9}\mu_{a2}(r)\varphi_2(r) = -\dfrac{2}{3}S(r) \end{cases} \tag{1}$$

where r is within the domain of the object, $\mu_{ai}(r) = \mu_a(r) + \mu_s(r)(1-g^i)$ and $\varphi_i(r)$ are the composites of the Legendre moments of radiance. $S(r)$ is the source term. For the excitation process, $S(r)$ denotes the known excitation light source. For the emission process, $S(r) = \Phi(r)X(r)$, where $\Phi(r)$ is the excitation light fluence and $X(r)$ is the fluorescent-yield distribution, which is unknown for the inverse problem. Equation (1) is complemented by the following boundary conditions:

$$\begin{cases} \left(\dfrac{1}{2} + A_1\right)\varphi_1(r) + \dfrac{1+B_1}{3\mu_{a1}(r)}\left(\vec{n}(r)\nabla\varphi_1(r)\right) \\ \quad = \left(\dfrac{1}{8} + C_1\right)\varphi_2(r) + \dfrac{D_1}{\mu_{a3}(r)}\left(\vec{n}(r)\nabla\varphi_2(r)\right) \\ \left(\dfrac{7}{24} + A_2\right)\varphi_2(r) + \dfrac{1+B_2}{7\mu_{a3}(r)}\left(\vec{n}(r)\nabla\varphi_2(r)\right) \\ \quad = \left(\dfrac{1}{8} + C_2\right)\varphi_1(r) + \dfrac{D_2}{\mu_{a1}(r)}\left(\vec{n}(r)\nabla\varphi_1(r)\right) \end{cases} \tag{2}$$

where r is on the boundary of the domain. The values of A_i, B_i, C_i, and D_i can be found in [9]. When practical measurement is taken, the measured quantity is the exiting partial current $J^+(r)$, which has the following form:

$$J^+ = \left(\frac{1}{4} + J_0\right)\varphi_1 - \left(\frac{0.5+J_1}{3\mu_{a1}}\right)\vec{n}\nabla\varphi_1 - \left(\frac{1}{16} + \frac{2J_0 - J_2}{3}\right)\varphi_2 - \left(\frac{J_3}{7\mu_{a3}}\right)\vec{n}\nabla\varphi_2. \tag{3}$$

The values of J_i can be found in [9]. By solving (2), $\vec{n}\nabla\varphi_i$ in (3) can be replaced with the linear combinations of φ_i.

B. Linear Relationship Establishment

In the finite-element framework, (1) and (2) are posed in their weak solution forms. By applying Green's first formula, the weak solution form of (2) can be integrated into the weak solution form of (1). After discretizing the domain with tetrahedron elements and employing the base functions as the test functions, φ_i can be approximated as $\varphi_i(r) \approx \sum_{p=1}^{N}\varphi_{i,p}\nu_p(r)$, where $\nu_p(r)$ is the base function for node p and $\varphi_{i,p}$ is the nodal value. N is the total number of the discretized nodes. Then, the SP_3 model can be linearized and the following matrix-form equation can be obtained:

$$\begin{bmatrix} M_{1\varphi_1} & M_{1\varphi_2} \\ M_{2\varphi_1} & M_{2\varphi_2} \end{bmatrix}\begin{bmatrix} \varphi_1 \\ \varphi_2 \end{bmatrix} = \begin{bmatrix} S \\ -\frac{2}{3}S \end{bmatrix}. \tag{4}$$

For the excitation process, the excitation light source is modeled as isotropic-point sources located one-mean-free path of photon transport beneath the surface. φ_1 and φ_2 can be directly obtained by solving (4). Considering the *inverse crime* problem, φ_1 and φ_2 are calculated on a fine mesh using second-order Lagrange elements. Then, the total fluence Φ, which is used as the energy source for the emission process, can be represented as $\varphi_1 - 2\varphi_2/3$ [11]. Next, we project Φ onto a coarse mesh which is used for the reconstruction of the fluorescent-source distribution with linear elements.

For the inverse problem, the unknown source term S is approximated as $S(r) \approx \sum_{p=1}^{N}\Phi_p X_p \nu_p(r)$, where X_p is the unknown nodal value of the fluorescent yield, which is to be reconstructed. Then, the following equation can be obtained:

$$\begin{bmatrix} M_{1\varphi_1} & M_{1\varphi_2} \\ M_{2\varphi_1} & M_{2\varphi_2} \end{bmatrix}\begin{bmatrix} \varphi_1 \\ \varphi_2 \end{bmatrix} = \begin{bmatrix} E_\Phi & 0 \\ 0 & E_\Phi \end{bmatrix}\begin{bmatrix} X \\ -\frac{2}{3}X \end{bmatrix}. \tag{5}$$

Based on (3) and (5), we can establish the linear relationship between the exiting partial current measurement J_m^+ and the unknown fluorescent yield distribution X as follows:

$$J_m^+ = AX. \tag{6}$$

C. Iteratively Reweighted Regularization

Due to the ill-posed and the ill-conditioned nature of the FMT problem, Tikhonov regularization is often utilized to make the solution more reasonable. Here, we extend Tikhonov regularization by incorporating a weighting matrix W

$$\min_{X\geq 0} E(X) = \frac{1}{2}\|AX - J_m^+\|_2^2 + \frac{\lambda^2}{2}\|WX\|_2^2 \tag{7}$$

where λ^2 is the regularization parameter that balances the two terms and W is a diagonal matrix. In this letter, we always assume that X is nonnegative. This energy function $E(X)$ can be efficiently minimized by iterative minimization tools such as the Newton method.

It is evident that the desirable norm $\|X\|_1$ can be represented using $\|WX\|_2^2$ by choosing W as follows:

$$W_1(i,i) = \begin{cases} \dfrac{1}{\sqrt{X(i)}}, & X(i) > 0 \\ 0, & X(i) = 0. \end{cases} \tag{8}$$

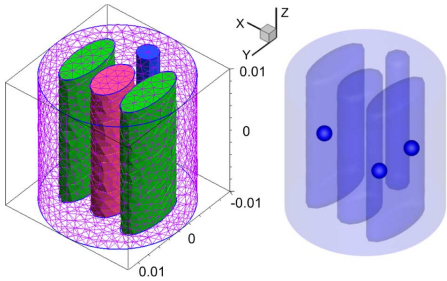

Fig. 1. Mouse-mimicking heterogeneous phantom with three spherical fluorescent sources of 2 mm in diameter centered in $z = 0$ plane.

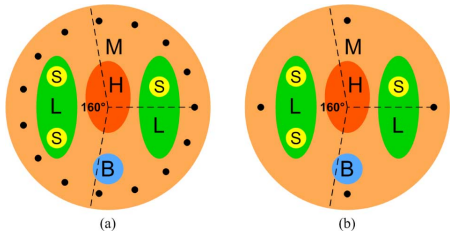

Fig. 2. Slice images of the phantom in $z = 0$ plane. The black dots in (a) and (b) represent the excitation point source locations. For each excitation location, fluorescence is measured from the opposite cylindrical side within 160° field of view.

However, W_1 depends on X which is unknown in advance. To resolve this problem, we assume that for every two adjacent iterations $n-1$ and n during the minimization process, $\|X_n - X_{n-1}\|_2$ is relatively small compared with $\|X_{n-1}\|_2$, which means that we can use X_{n-1} to approximate X_n to some extent. Therefore, for every new iteration n, we can construct the sparsity-promoting regularizer $\|X\|_1$ using the current solution X_{n-1}. Based on this, we redefine the weighting matrix W_1 as follows to approximate L1-norm regularization, which is termed as L1-like regularization:

$$W_1(i,i) = \begin{cases} \dfrac{1}{\sqrt{X_{n-1}(i)}}, & X_{n-1}(i) > 0 \\ 0, & X_{n-1}(i) = 0 \end{cases} \tag{9}$$

where X_{n-1} is the solution from the last iteration.

For the first few iterations of the minimization algorithm, the solution X_n may vary rapidly, which violates our basic assumption. To resolve this problem, Tikhonov regularization is firstly used for several iterations to provide a rough initial guess. The number of iterations can be set in advance using empirical data or be determined dynamically depending on $\|X_n - X_{n-1}\|_2 / \|X_{n-1}\|_2$. Then, L1-like regularization starts from the initial guess to compute a sparse solution.

III. Simulation Results

In this section, heterogeneous-simulation experiments were conducted to verify the sparsity-promoting characteristic of the proposed method. Fig. 1 shows the heterogeneous-cylindrical phantom we used, which was of 20 mm in diameter and 20 mm in height. The phantom consisted of four kinds of materials, which is illustrated in Fig. 2, to represent muscle (M), lung (L), heart (H), and bone (B), respectively. The optical parameters can be found in Table I, where subscripts x and m denote the excitation and emission wavelengths, respectively. The anisotropy parameter g was set to be 0.85. Three spherical-fluorescent sources of 2 mm in diameter centered in $z = 0$ plane were placed in the left and the right lungs. The fluorescent yield was set to be 0.5.

Fluorescence measurement was implemented in transillumination mode. For each excitation source, which was modeled as an isotropic point source located one-mean-free path of photon transport beneath the surface in $z = 0$ plane, measurement of the emitted fluorescence on the surface was taken from the opposite cylindrical side within 160° field of view (FOV), which is illustrated in Fig. 2. It means that all the nodes on the cylindrical side within this FOV were considered to be measurable.

TABLE I
Optical Parameters of Phantom (Unit: mm^{-1})

Material	μ_{ax}	μ_{sx}	μ_{am}	μ_{sm}
Muscle	0.0849	4.27	0.0563	3.79
Lung	0.1918	21.72	0.1266	21.24
Heart	0.0574	9.62	0.0383	9.05
Bone	0.0594	24.90	0.0393	23.40

The Newton method was adopted to iteratively compute the solution. To provide an initial guess, the Tikhonov method was used for the first ten iterations. Then, L1-like regularization proceeded the reconstruction from the initial guess. The regularization parameter λ^2 plays an important role in the FMT reconstructions. However, finding the optimal λ^2 is itself a very challenging task and will not be covered in this letter. Instead, we sampled the range between 1e-8 and 1e-13 which was sufficient for this experiment, and performed reconstructions using these sampled values. The best value for λ^2 was chosen by visual inspection of the results and quantitative comparisons between the reconstructed location errors.

In the first experiment, the fluorescence was excited by point sources from 15 different locations in sequence, which is illustrated in Fig. 2(a). Measurements were taken every 24° and a total of 15 datasets were acquired for the reconstruction of the fluorescent yield. To show the merits of the proposed method, L1-like regularization was compared with the Tikhonov method. Fig. 3 shows the reconstruction results, which are presented in the form of slice images in $z = 0$ plane and isosurfaces for 30% of the maximum value. The small circles in the slice images denote the real positions of the fluorescent sources. From Fig. 3, we can clearly see that the result obtained using the Tikhonov regularization is slightly over-smoothed with reduced intensities. On the contrary, the L1-like regularization can better preserve the sparsity of the fluorescent sources, and the reconstructed intensities are greater.

Next, we reduced the amount of measurement data to simulate a much worse case. This is possible when long-time measurement is not appropriate or feasible. For instance, when imaging small animals like mice, the artifacts caused by movements must be taken into consideration. Besides, long-time measurement can cause the bleaching effect of the fluorescent probes and affect the accuracy of the reconstruction results. One way to resolve this problem is to reduce the number of fluorescence measurements. This requires that we should be able to

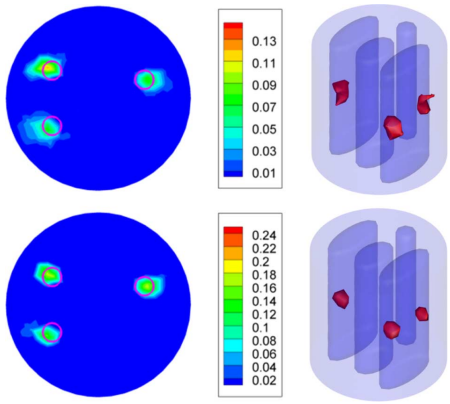

Fig. 3. Reconstruction results using 15 measurement datasets with Tikhonov regularization (first row) and L1-like regularization (second row). These results are presented in the form of slice images in $z = 0$ plane (left column) and isosurfaces for 30% of the maximum value (right column). The small circles in the slice images denote the real positions of the fluorescent sources.

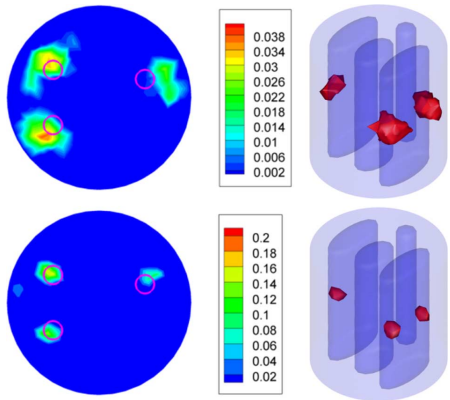

Fig. 4. Reconstruction results using four measurement datasets with Tikhonov regularization (first row) and L1-like regularization (second row). These results are presented in the form of slice images in $z = 0$ plane (left column) and isosurfaces for 30% of the maximum value (right column). The small circles in the slice images denote the real positions of the fluorescent sources.

reconstruct the fluorescent sources from very limited data. It has been shown in bioluminescence tomography that, by using L1-norm regularization, satisfactory results can still be achievable even with very limited imaging data [3]. Here, we only used four measurement datasets, which is illustrated in Fig. 2(b). Fig. 4 shows the reconstruction results using Tikhonov regularization and the proposed method. From these results, we can clearly see that due to the badly ill-posed situation, the reconstruction result from the Tikhonov method is seriously over-smoothed. However, the proposed method can still preserve the sparsity of the sources very well. This demonstrates the applicability of the proposed method under more ill-posed conditions.

IV. Conclusion

In this paper, the SP_3 approximation to RTE has been utilized to model the photon transport within heterogeneous biological tissues. Considering the sparsity characteristic of the fluorescent sources, we have proposed a sparsity-promoting regularization method for the FMT reconstructions. This method is based on an iteratively reweighted scheme, which can approximate L1-norm regularization. The advantage of the proposed method is that it can be easily incorporated into the existing iterative reconstruction framework, and the extra work is merely the construction of a diagonal weighting matrix at each iteration, which is a relatively cheap operation. For the evaluation of this method, heterogeneous-simulation experiments have been conducted. Compared with the Tikhonov method, more reasonable and satisfactory results can be obtained when using L1-like regularization, even with very limited measurement data. This demonstrates the applicability of the proposed method for the early detection of tumors, which are usually small and sparse at this stage. Of course, there are situations in which the assumption that the solution will be sparse cannot hold, e.g., a large tumor or broadly distributed fluorescence signals, and the proposed method may fail in those cases.

For FMT reconstruction, the choice of the regularization parameter will have a significant impact on the results. A large parameter value can make the reconstructed solution deviate from the real distribution, while a small value will have little contribution to the regularization of the problem. Finding the optimal or near-optimal regularization parameter automatically still remains a challenging task. Generally speaking, two strategies can be used: determining the parameter in advance or updating it heuristically. This will be our future research.

In conclusion, we have developed a sparsity-promoting reconstruction method for FMT. Numerical simulations show the merits of our method. *In vivo* mouse studies using the proposed method will be reported in the future.

References

[1] V. Ntziachristos, J. Ripoll, L. V. Wang, and R. Weissleder, "Looking and listening to light: The revolution of whole-body photonic imaging," *Nat. Biotechnol.*, vol. 23, no. 3, pp. 313–320, 2005.

[2] J. Tian, J. Bai, X. Yan, S. Bao, Y. Li, W. Liang, and X. Yang, "Multimodality molecular imaging," *IEEE Eng. Med. Biol. Mag.*, vol. 27, no. 5, pp. 48–57, Sep./Oct. 2008.

[3] Y. Lu, X. Zhang, A. Douraghy, D. Stout, J. Tian, T. F. Chan, and A. F. Chatziioannou, "Source reconstruction for spectrally-resolved bioluminescence tomography with sparse *a priori* information," *Opt. Exp.*, vol. 17, no. 10, pp. 8062–8080, 2009.

[4] P. Mohajerani, A. A. Eftekhar, J. Huang, and A. Adibi, "Optimal sparse solution for fluorescent diffuse optical tomography: Theory and phantom experimental results," *Appl. Opt.*, vol. 46, no. 10, pp. 1679–1685, 2007.

[5] D. L. Donoho and X. Huo, "Uncertainty principles and ideal atomic decomposition," *IEEE Trans. Inf. Theory*, vol. 47, no. 7, pp. 2845–2862, Nov. 1999.

[6] E. Candes, J. Romberg, and T. Tao, "Stable signal recovery from incomplete and inaccurate measurements," *Commun. Pure Appl. Math.*, vol. 59, no. 8, pp. 1207–1223, 2005.

[7] J.-C. Baritaux, M. Guerquin-Kern, and M. Unser, "Integrated modeling and reconstruction with sparsity constraints for fDOT," in *Proc. IEEE Int. Symp. Biomed. Imag.*, 2009, pp. 173–176.

[8] N. Cao, A. Nehorai, and M. Jacob, "Image reconstruction for diffuse optical tomography using sparsity regularization and expectation-maximization algorithm," *Opt. Exp.*, vol. 15, no. 21, pp. 13695–13708, 2007.

[9] A. D. Klose and E. W. Larsen, "Light transport in biological tissue based on the simplified spherical harmonics equations," *J. Comput. Phys.*, vol. 220, no. 1, pp. 441–470, 2006.

[10] Y. Lu, A. Douraghy, H. B. Machado, D. Stout, J. Tian, H. Herschman, and A. F. Chatziioannou, "Spectrally resolved bioluminescence tomography with the third-order simplified spherical harmonics approximation," *Phys. Med. Biol.*, vol. 54, no. 21, pp. 6477–6493, 2009.

[11] M. Chu and H. Dehghani, "Image reconstruction in diffuse optical tomography based on simplified spherical harmonics approximation," *Opt. Exp.*, vol. 17, no. 26, pp. 24208–24223, 2009.

[12] I. F. Gorodnitsky and B. D. Rao, "Sparse signal reconstruction from limited data using FOCUSS: A re-weighted minimum norm algorithm," *IEEE Trans. Signal Process.*, vol. 45, no. 3, pp. 600–616, Mar. 1997.